

AD No.
 ODC FILE COPY

AD A051189

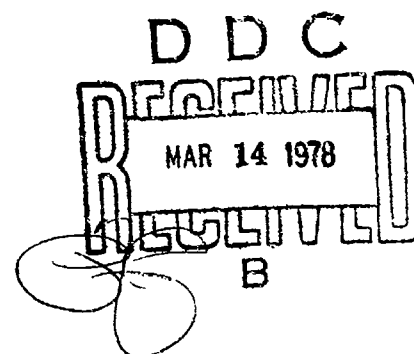
RADC-TR-77-285
IN-HOUSE REPORT
AUGUST 1977



2
S
C

Measured Backscatter Modulation From Linearly Oscillating Metal Disks

RICHARD B. MACK



Approved for public release; distribution unlimited.

ROME AIR DEVELOPMENT CENTER
AIR FORCE SYSTEMS COMMAND
GRIFFISS AIR FORCE BASE, NEW YORK 13441

This report has been reviewed by the RADC Information Office (OI) and is releasable to the National Technical Service (NTIS). At NTIS it will be releasable to the general public, including foreign nations.

This technical report has been reviewed and approved for publication.

APPROVED:



PHILIPP BLACKSMITH
Chief, Antenna and Radar Techniques Branch

APPROVED:



ALLAN C. SCHELL
Acting Chief
Electromagnetic Sciences Division

FOR THE COMMANDER:



Plans Office

Unclassified

SECURITY CLASSIFICATION OF THIS PAGE (When Data Entered)

REPORT DOCUMENTATION PAGE		READ INSTRUCTIONS BEFORE COMPLETING FORM
1. REPORT NUMBER RADC-TR-77-285	2. GOVT ACCESSION NO.	3. RECIPIENT'S CATALOG NUMBER
4. TITLE (and Subtitle) MEASURED BACKSCATTER MODULATION FROM LINEARLY OSCILLATING METAL DISKS		5. TYPE OF REPORT & PERIOD COVERED Inhouse
7. AUTHOR(s) Richard B. Mack		6. PERFORMING ORG. REPORT NUMBER
9. PERFORMING ORGANIZATION NAME AND ADDRESS Deputy for Electronic Technology (RADC) ✓ Hanscom AFB Massachusetts 01731		10. PROGRAM ELEMENT, PROJECT, TASK AREA & WORK UNIT NUMBERS 61102F 2305J403
11. CONTROLLING OFFICE NAME AND ADDRESS Deputy for Electronic Technology (RADC) Hanscom AFB Massachusetts 01731		12. DATE Aug 77
14. MONITORING AGENCY NAME & ADDRESS (if different from Controlling Office)		13. NUMBER OF PAGES 24
		15. SECURITY CLASS. (of this report) Unclassified
16. DISTRIBUTION STATEMENT (of this Report) Approved for public release, distribution unlimited.		15a. DECLASSIFICATION/DOWNGRADING SCHEDULE
17. DISTRIBUTION STATEMENT (of the abstract entered in Block 20, if different from Report)		
18. SUPPLEMENTARY NOTES		
19. KEY WORDS (Continue on reverse side if necessary and identify by block number) Radar signatures Oscillating targets Experimental equipment Scattered field modulation Phase modulations		
20. ABSTRACT (Continue on reverse side if necessary and identify by block number) The work described in this report was carried out as part of the basic research program directed toward providing an understanding of the radar detection of agitated metals (RADAM). The report describes an experimental equipment and measurement procedure that permits determination of the kind and amount of modulation introduced onto the backscattered electromagnetic signal by a vibrating or oscillating scattering target. Although discussed specifically in terms of equipment realization at 10 GHz, the techniques are		

DD FORM 1 JAN 73 1473 EDITION OF 1 NOV 65 IS OBSOLETE

Unclassified
SECURITY CLASSIFICATION OF THIS PAGE (When Data Entered)

309 050 Doc

Unclassified

SECURITY CLASSIFICATION OF THIS PAGE(When Data Entered)

20. Abstract (Continued)

general. Provision has been included for determining characteristics of the mechanical motion and correlating mechanical and electromagnetic results in the time and frequency domain.

The results of a series of measurements of modulated backscatter cross sections due to a disk executing small rigid translational oscillations show the modulation introduced to be all phase modulation; measured results are in good agreement with those calculated from a soundly-based theory. In addition, it is shown that the modulation amplitude is independent of modulation frequency, that the phase modulation introduced is directly proportional to the amplitude of the mechanical oscillation, and that the spectral components of the modulated signal are monotonically decreasing for simple sinusoidal motion.

Unclassified

SECURITY CLASSIFICATION OF THIS PAGE(When Data Entered)

Preface

The author gratefully acknowledges numerous helpful and stimulating discussions with Professor R. E. Kleinman of the University of Delaware, and the assistance of Mr. G. H. Preston, who assembled the experimental equipment and assisted with the measurements.

ACCESSION for		
NTIS	White Section	<input checked="" type="checkbox"/>
DDC	Buff Section	<input type="checkbox"/>
UNANNOUNCED		<input type="checkbox"/>
JUSTIFICATION _____		
BY _____		
DISTRIBUTION/AVAILABILITY CODES		
Dist.	AvAIL. and / or	SPECIAL
A		

Contents

1. INTRODUCTION	7
2. EQUIPMENT AND MEASUREMENT PROCEDURES	8
3. MEASURED MODULATION PROPERTIES	18
REFERENCES	24

Illustrations

1. Measuring Equipment for Phase and Amplitude Modulation Study	9
2. Tunnel Antennas for Transmitting and Receiving	11
3. The Vibrator, Scattering Disk, Driving Sources, and Vibration Meter	13
4. Vibrator, Disk, and Tunnel Antennas	13
5. Transmitting and Receiving Equipment	14
6. D-c Output from Phase Section of Receiver vs Phase Differences of Input Signals	14
7. Sample Outputs from Amplitude Modulation Section of Receiving Equipment	15
8. Comparison of Scattered Phase Waveform with Waveform of Mechanical Motion ($f = 20$ Hz)	15
9. Disk Motion with Nonsinusoidal Driving Waveform	16

Illustrations

10. (a) Backscattered RCS of Disk. (b) Backscattered Phase of Disk	17
11. Measured Phase and Amplitude Modulations for Three Vibration Amplitudes	19
12. Phase Modulation from Constant Displacement Amplitude, Differing Vibration Frequencies	20
13. Measured Phase Modulation vs Vibrational Amplitude	21
14. Modulation Spectra for Sinusoidal Oscillation of Target	23
15. Comparison of Measured and Calculated Spectral Levels for Sinusoidal Vibration	24

Measured Backscatter Modulation From Linearly Oscillating Metal Disks

I. INTRODUCTION

This technical report describes the results of an experimental investigation of the changes produced in the backscattered electromagnetic field by a disk that is undergoing rigid translational oscillations along its axis. A scattering target which is experiencing such vibrational motion operates, in effect, as an external mechanical modulator of the reflected radar beam, introducing a spectral broadening with specific features that are determined by the form, frequency, and amplitude of the mechanical motion.

A scattering target which is experiencing periodic rigid translational motion may be considered as a typical basic component of more complicated assemblies such as complete trucks or tanks. Thus, although the investigation was confined to one specific scatterer for experimental convenience, a number of inferences having quite general applications can be drawn from the results.

The work to be described herein was one of a series of laboratory studies directed toward exploring the radar detection of agitated metals (RADAM) phenomenon. Early investigations of RADAM raised a number of questions concerning the characteristics of more conventional sources of modulation of the radar cross sections of complex scatterers such as vehicles. A knowledge of the spectral characteristics introduced by potential sources of conventional modulations

(Received for publication 22 August 1977)

facilitated the interpretation of the complex spectra from field measurements that contained superimposed effects from a large variety of modulation sources.

The measurements were carried out at 10 GHz using a CW backscatter equipment that was modified to permit a determination of the type of modulation introduced and separate investigations of spectra due to phase and amplitude modulations. The experiment was instrumented to permit simultaneous observation of the mechanical motion and its spectrum, as well as the resulting electromagnetic effects. The scattering target was mounted on a low force vibration calibrator whose frequency and displacement could be accurately controlled. The vibration calibrator, together with its target, was mounted on a rigid tripod; the assembly was covered with radar-absorbing material and placed in a microwave anechoic chamber to simulate free-space conditions.

The scattering target was a 5-3/4 in. diam disk of 1/8 in. thick aluminum. In terms of the wavelength, it was 0.106λ in thickness and 4.873λ in diameter, corresponding to $ka = 15.309$, where $k = 2\pi/\lambda$ and a is its radius.

2. EQUIPMENT AND MEASUREMENT PROCEDURES

A conventional 10-GHz CW backscatter equipment¹ formed the basis of the measuring equipment. Modifications included the use of separate antennas for transmitting and receiving, and the provision of separate channels for examining the spectral characteristics due to amplitude modulation and those due to phase or frequency modulation. A block diagram of the final form of the equipment is given in Figure 1.

As shown in Figure 1, the equipment was divided into five sections: (1) a transmitting section, (2) a receiving section through the hybrid tee, (3) a section responding only to phase modulation, (4) a section responding only to amplitude modulation, and (5) a section indicating the total modulation waveform and spectrum, regardless of the type of modulation. The fifth section was basically a homodyne receiver operating at 30 MHz; its output approximates most closely the output from typical homodyne radars used for full-scale field measurements.

The transmitter consisted of a Varian X-13 klystron with a H.P. Model 716B Klystron Power Supply, phase stabilized by a FEL Model 133-A Phase Lock Synchronizer. Typical output through a high-directivity uniline was 500 to 750 MW. The uniline helped in stabilizing output of the X-13 tube by largely isolating it from adjustments or mismatches at the antenna, or in the phase comparison sections of

1. Maek, R. B., Wojcieki, A. W., and Andriotakis, J. J. (1973) An Implementation of Conventional Methods of Measuring the Amplitude and Phase of Backscatter Fields, AFCHL-TR-73-0418.

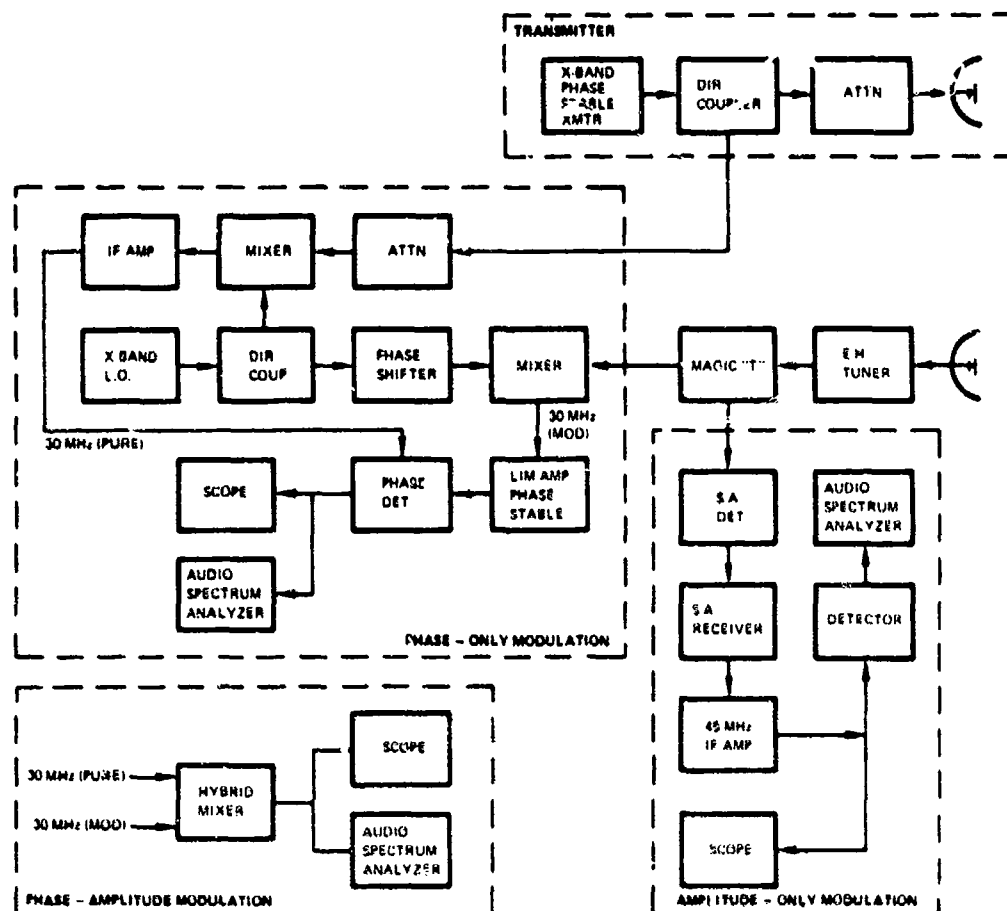


Figure 1. Measuring Equipment for Phase and Amplitude Modulation Study

the equipment. In addition to the usual signal samples for amplitude and frequency monitoring (not shown in Figure 1), a small fraction of the transmitted power was also extracted for the phase comparison reference.

Phase comparison was done at 30 MHz. To beat the X-band signals down to 30 MHz, an LFE Model 814A-X-21 Ultrastable Microwave Oscillator tuned to $10 \text{ GHz} + 30 \text{ MHz}$ was used as a local oscillator. Two reference signals were extracted from the local oscillator through a directional coupler and appropriate level set attenuators: One of these signals was mixed with the phase reference from the transmitter to yield a 30-MHz "pure" signal having no modulation; the second reference signal from the local oscillator was mixed with a sample of the power from the scattering target to yield a 30-MHz signal that contained any modulation introduced by the scatterer. Amplitude variations introduced by the target

were removed by feeding the 30-MHz signal from the receiver through a phase-stable limiting amplifier. Finally, phase information was extracted by feeding the pure 30-MHz reference signal and the 30-MHz amplitude-limited signal containing target information to an H. P. Model 10514A Mixer/Phase Detector.

In order to obtain an output showing amplitude modulation independent of phase modulation or frequency modulation, advantage was taken of the wide frequency differences between a 45 MHz i-f and typical modulation frequencies of the order of tens or hundreds of cycles, and of the inability of an oscilloscope to resolve simultaneously both the modulation frequency and the i-f frequency. High r-f sensitivity was obtained by feeding approximately one-half of the received signal through a Scientific Atlanta (SA) Model 13A waveguide mixer to an SA Model 1750 Wide Range Phase/Amplitude Receiving System. The signal was then extracted from the receiver at the 45 MHz i-f stage and routed through a 45 MHz i-f amplifier to the oscilloscope, audio spectrum analyzer, or other instrument for analysis. Various spectrum analyzers used for analysis of both amplitude and phase included Tektronix Model 11.5 plug-in adaptor in Tektronix Model 581 oscilloscopes, as well as an H. P., Model 3380A Spectrum Analyzer. An H. P. Model 302A Wave Analyzer was also used. This was particularly useful at the lowest modulation frequencies since the Model 11.5 had a lower frequency limit of about 20 Hz, whereas the Model 302A performed well down to 1 Hz.

With no amplitude modulation, the oscilloscope display from the amplitude section was simply a filled space between straight top and bottom lines. Amplitude modulation at the low audio rates appeared as a scalloping of the top and bottom lines. The percentage of amplitude modulation present in the unknown scattering signal was determined by successively displaying the scattering signal and one at 45 MHz from a H. P. Model 8640B Frequency Synthesizer fed through the 45-MHz i-f amplifier to the oscilloscope. The calibrated percentage of amplitude modulation of the latter signal was adjusted to produce the same display as that of the unknown and the percentage of modulation read from the Model 8640B Frequency Synthesizer. Amplitude modulations as small as 1/2 percent or less could readily be observed.

When the entire modulation spectrum was desired, regardless of the kind of modulation, the 30-MHz scattered signal was mixed without amplitude limiting or other prior conditioning with the 30-MHz reference signal. Depending on its amplitude, the output from the mixer was either displayed on the desired signal analyzer directly, or amplified and displayed.

In order to reduce spillover and leakage coupling to levels sufficiently below the signal levels from the scattering targets for reliable measurements, tunnel antennas were used for transmitting and receiving. These antennas were basically 6 in. diam paraboloidal reflectors with conventional double dipole feeds; the

reflector and feed assemblies were placed inside cylinders formed by 8-in. diam stovepipe lined with AN/75 absorber (Figure 2). The rear of the cylinders was electrically closed with aluminum foil and conducting tape, sealed to both the tube and the waveguide feed. The best distance of the reflector from the radiating aperture of the tunnel was determined experimentally and found to be about 3-1/2 in. for the combinations of interest here. The best distance was taken to be the one that gave greatest reduction of far-out sidelobes without reducing the antenna gain and broadening the main beam. This location resulted in half power beam widths of about 14° and highest sidelobes of about -17 dB for the combinations listed above. The use of the tunnel reduced antenna lobes and spillover by 15 to 25 dB over all angular regions beyond $\pm 36^\circ$ of the main beam.

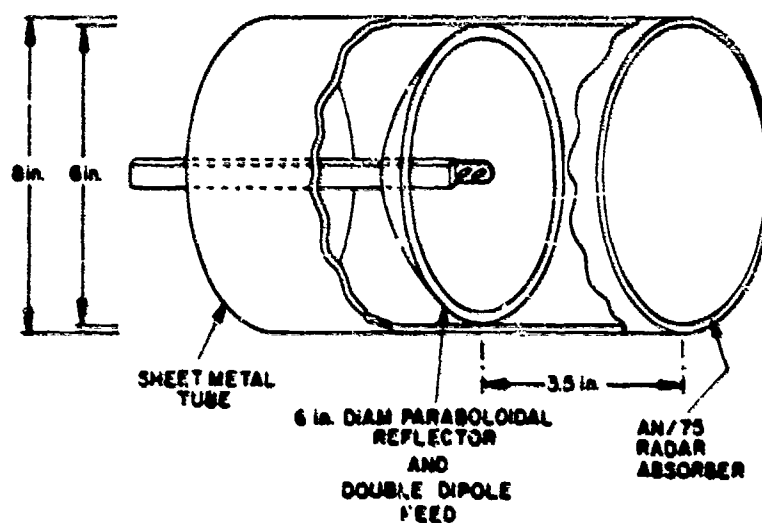


Figure 2. Tunnel Antennas for Transmitting and Receiving

The scattering models to be measured were mounted on a LTV-Ling Electronics Model 6C Vibrator Calibrator. This vibrator has a maximum force rating of 25 lb and a frequency range between 5 Hz and 2 KHz. With this vibrator, the form of the motion was strongly sinusoidal for the displacements of primary interest. An external function generator, Wavetek Model 105, was generally used as a driver. Motion characteristics were determined with a General Radio Model 1553A Vibration Meter. The associated mechanical pickup, General Radio Model 1525-P2, was mounted behind the disk, and electrical cables were arranged

to minimize their interference. The vibrator was covered with microwave absorber and its tripod mount shielded by a panel of absorber to reduce this source of interfering reflections; the entire assembly was located in a microwave anechoic chamber to approximate free-space measuring conditions. With this arrangement, displacement amplitudes could be controlled to approximately ± 0.002 in., or $\pm 0.6^\circ$, of phase and vibration frequencies to a few hertz.

The vibrator with a scattering disk mounted, its power supply, the Wavetek function generator, and the General Radio Vibration Meter are shown in Figure 3. When measurements were being made, only the vibrator and its mount were in the chamber. Figure 4 shows the vibrator and scattering disk along with the tunnel antennas used for transmitting and receiving. The transmitting and receiving systems are located in a separate room behind the antennas, as shown in Figure 5; also in Figure 5, the X-13 transmitting tube is located behind the shield of the receiving screen of the oscilloscope; the SA Receiver is not shown.

A typical output from the phase detector is shown in Figure 6. Here, the phase of one signal was held constant whereas the phase of the other was changed in discrete steps by means of an HP Model X885-A waveguide phase shifter. For each setting, the relative d-c output level was read on an oscilloscope. As can be seen from Figure 6, the central portion of the response curve is linear. Phase data were taken on this portion of the curve by adjusting the waveguide phase shifter until the maximum deviations of the phase waveform fell successively on the central horizontal line of the oscilloscope display; the phase was then determined from the difference in readings of the phase shifter for the two adjustments.

Examples of the output from the amplitude modulation section of the receiving system are shown in Figure 7. The oscilloscope time domain displays resulted from a 45-MHz signal from the Model 8640B signal generator being fed through the i-f section of the equipment with known amounts of amplitude modulation. From Figure 7(b) it is clear that amplitude modulations of 1 percent or less could easily be detected.

As long as total phase excursions were restricted to the linear portion of the phase detector, the output waveform of the phase analysis section of the receiver followed that of the motion. For example, the bottom curve of Figure 8 shows an oscilloscope trace (amplitude vs time) of the output of the mechanical vibration pickup and vibration meter. In this particular example, the disk was moving with a sinusoidal motion at a frequency of 20 Hz with a maximum displacement of $kd = 3/4$, where $k = 2\pi/\lambda$ and d is the peak-to-peak displacement. The curve at the top of Figure 8 is a corresponding oscilloscope trace of the output of the phase detector for the same motion of the disk, showing the waveform of the motion to be faithfully reproduced by the scattered radar signal.

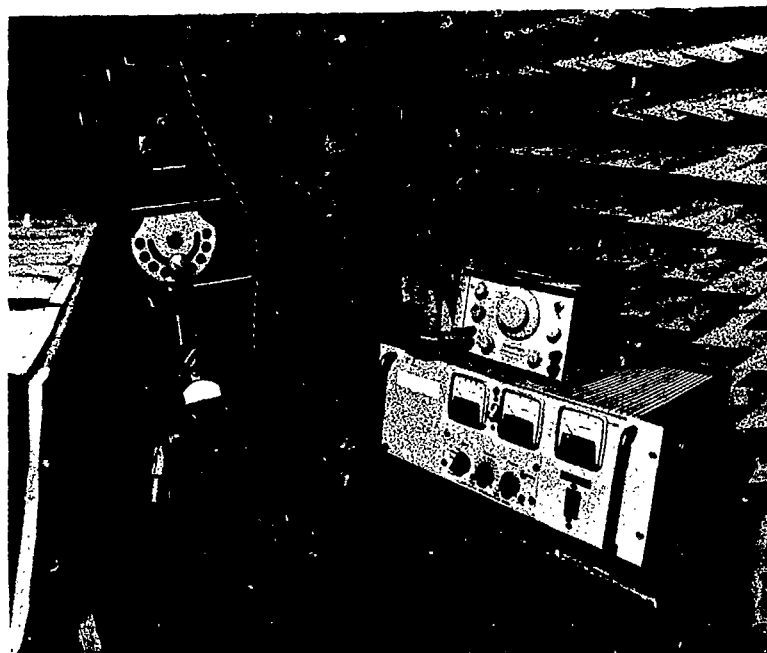


Figure 3. The Vibrator, Scattering Disk, Driving Sources, and Vibration Meter

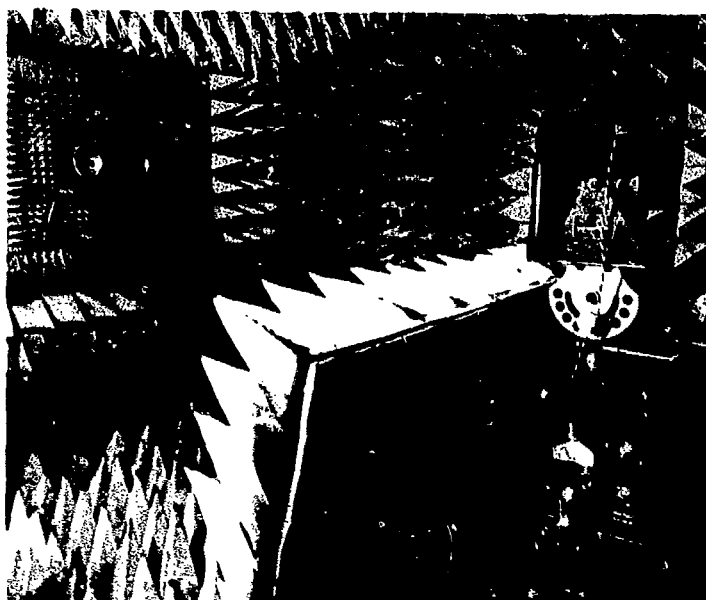


Figure 4. Vibrator, Disk, and Tunnel Antennas

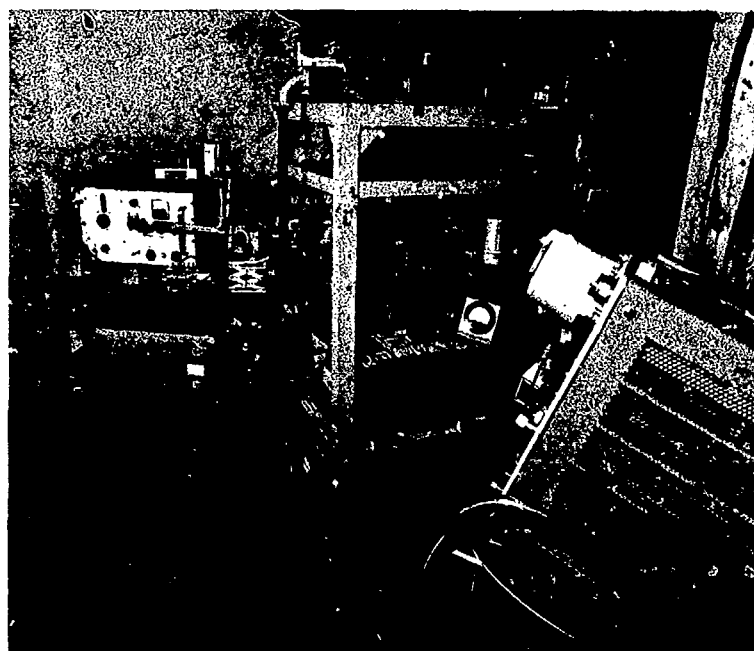


Figure 5. Transmitting and Receiving Equipment

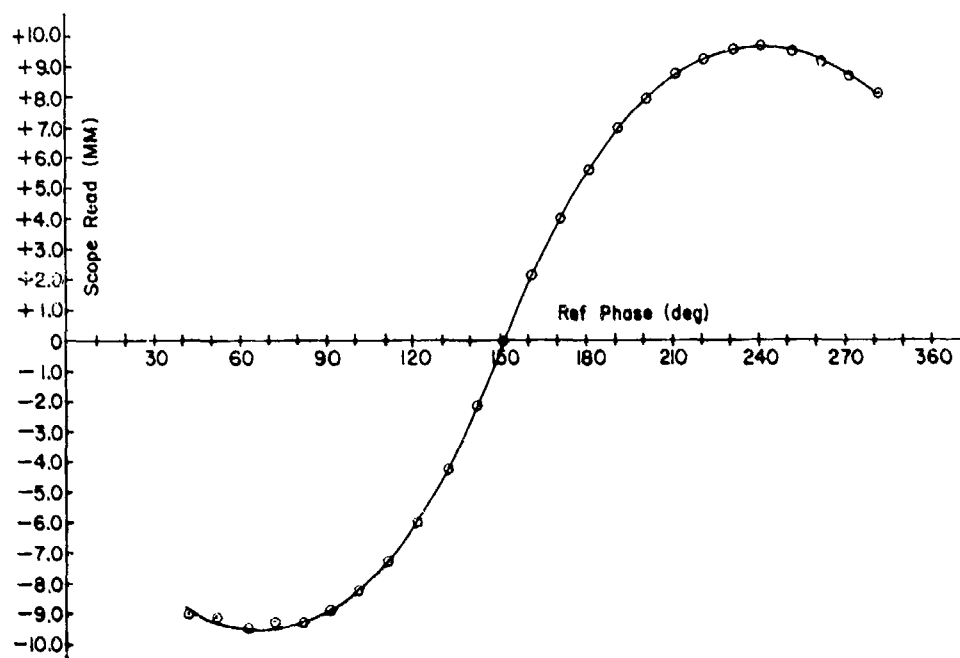


Figure 6. D-c Output from Phase Section of Receiver vs Phase Differences of Input Signals

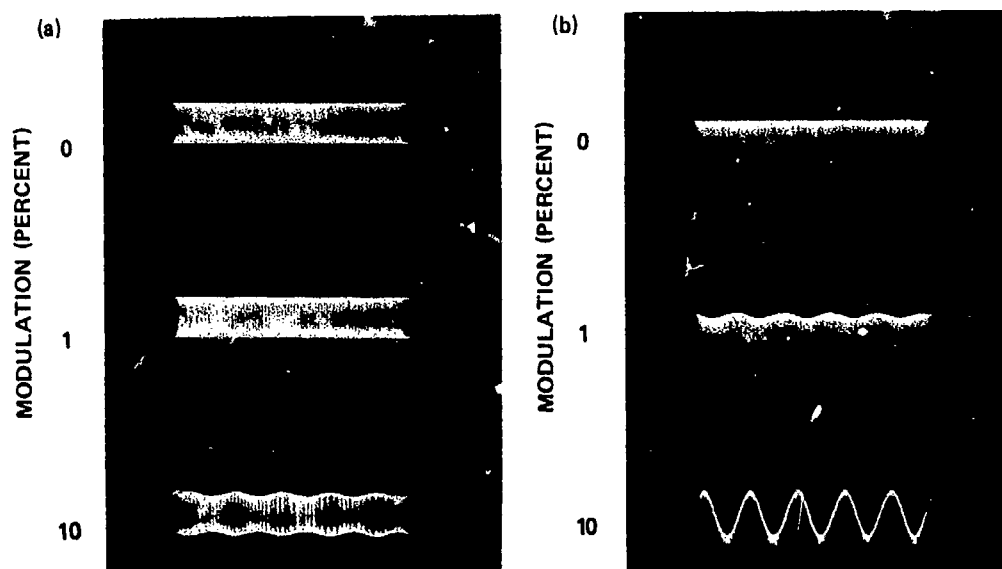


Figure 7. Sample Outputs from Amplitude Modulation Section of Receiving Equipment. (a) Regular display. (b) Expanded display

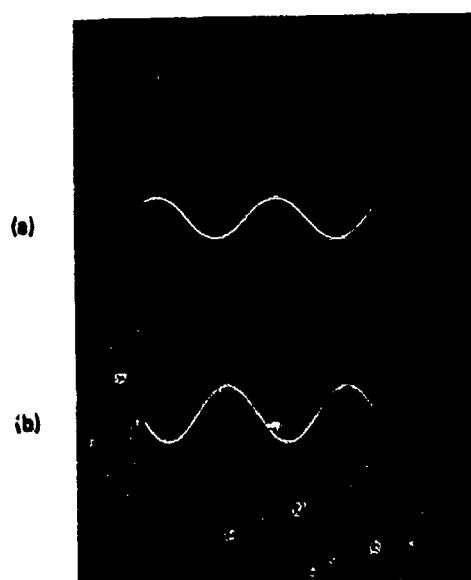


Figure 8. Comparison of Scattered Phase Waveform with Waveform of Mechanical Motion ($f = 20$ Hz). (a) Waveform from phase detector. (b) Waveform from mechanical pickup. (Relative amplitude vs. time display)

The design of the vibrator tended to force a sinusoidal motion response regardless of the driving waveform. Figure 9 shows the results of an attempt to drive the disk with a triangular waveform. Again, the displacement was $k_d = 3/4$, but the frequency was reduced to 5 Hz, in order to permit longer motion response times.

The bottom curve of Figure 9 shows the driving waveform from the Wavetek function generator. Figure 9(b) is the output of the vibration pickup, showing the actual form of the motion being executed by the disk. Finally, Figure 9(a) shows the output of the phase detector. As can be seen, this curve closely follows the distorted sinewave of the actual motion, but the motion does not closely follow the driving function.

Conventional backscatter-RCS and phase patterns are given in Figure 10(a) and (b), respectively. Some asymmetry is evident in the RCS pattern of Figure 10(a) but it is much more clearly displayed in the phase pattern of Figure 10(b). This was traced to the GR Model 1560-P2 vibration pickup mounted near one edge of the disk that directly contributed to the scattered field, beginning at angles near 10° for CW rotations.

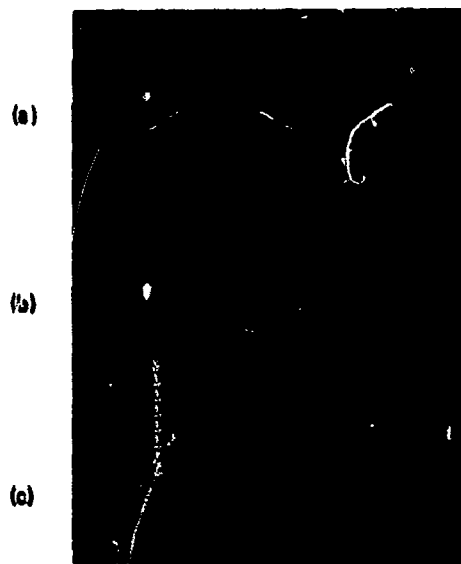


Figure 9. Disk Motion with Nonsinusoidal Driving Waveform. (a) Scattered phase. (b) Response (actual motion). (c) Driving waveform. (Relative amplitude vs time display)

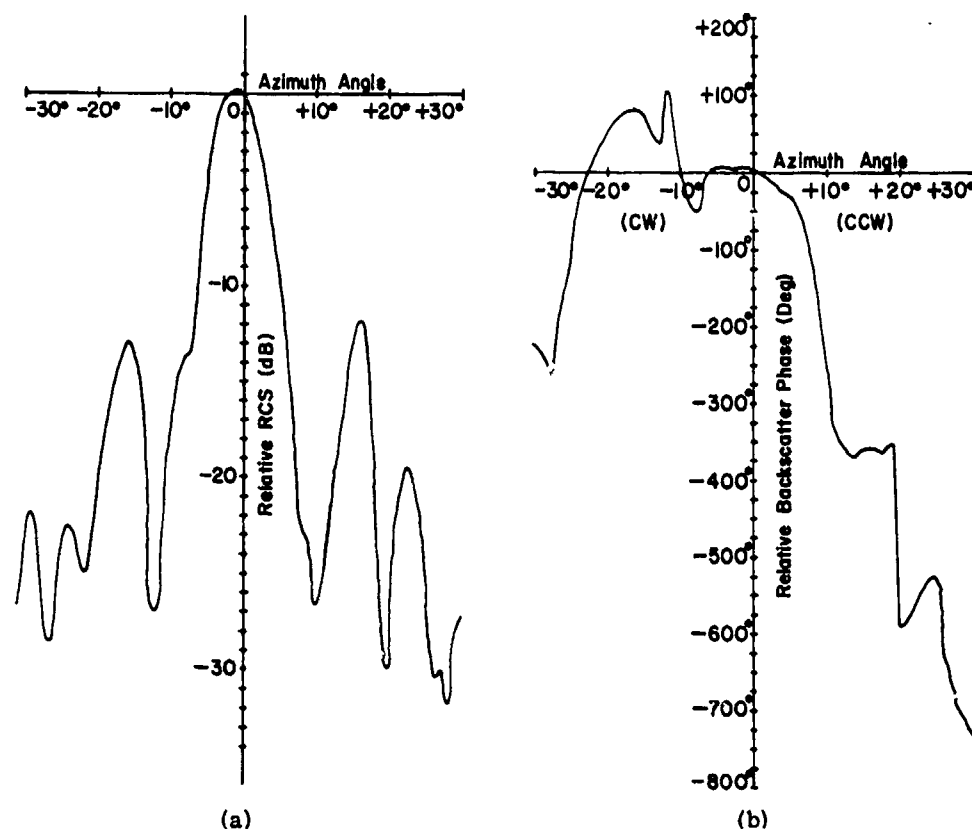


Figure 10. (a) Backscattered RCS of Disk. (b) Backscattered Phase of Disk

Since the disk was mounted 5.75 in. forward of the center of rotation of the mount, a correction has been provided in the phase measurements to compensate for the motion of the disk away from the antennas, as it was rotated. The correction was calculated from

$$\phi_{\text{corr}} = 720 \, l / \lambda \quad (1)$$

$$l = 5.75 \text{ in. } (1 - \cos \theta) \quad (2)$$

where θ is the azimuth angle of rotation, λ the wavelength, and l is the amount of movement from the normal orientation.

The results as shown in Figure 10 were obtained from point-by-point measurements using the Scientific Atlanta Model 1750 and Amplitude Receiver in its conventional operational mode.

3. MEASURED MODULATION PROPERTIES

This section contains the results of several measurements designed to illustrate specific properties of the modulations introduced by linear translational oscillations of the scattering targets. In particular, it will be shown (a) that the modulation introduced by such motion is phase modulation; (b) that the modulation amplitude is independent of the modulation frequency; (c) that the phase modulation introduced is directly proportional to the amplitude of the mechanical oscillation; (d) that the spectral components of the modulated signal are monotonically decreasing for simple sinusoidal motion; and (e) that the measured results are in good agreement with corresponding results calculated from a soundly-based theoretical model. In addition, it will be shown that the amplitude of the spectral components exhibits a high degree of aspect invariance when measured with the system described in Section 2.

Figure 11 shows the output of the separate receiver sections that were designed to respond only to amplitude modulation or to phase modulation. Parts (a), (b), and (c) are results for peak-to-peak vibrational amplitudes of 0.071 inch, 0.155 inch, and 0.310 inch, corresponding to $\lambda/16$, $\lambda/8$, and $\lambda/4$ respectively. Because of the two-way path of the scattered signal, these vibrational amplitudes result in phase changes of 45° , 90° , and 180° , respectively. Each trace in the figure is a conventional amplitude versus time display. The top trace of each set is the output of the amplitude-sensitive section; the bottom trace, the output of the phase-sensitive section; and the middle trace, the output from the amplitude-sensitive section with a calibrated input to determine the degree of amplitude modulation, as discussed in Section 2.

Figure 11(a), (b), and (c) clearly show that the vibrating target introduces predominantly phase modulation; there is no measurable amplitude modulation for vibrational amplitudes that produce up to 45° phase modulation. Ninety degrees of phase modulation, Figure 11(b), is accompanied by approximately 1/2 percent amplitude modulation, whereas 180° of phase modulation, Figure 11(c), is accompanied by approximately 4 percent amplitude modulation.

For these measurements, the disk was located approximately 90 in. from the transmitting and receiving antennas. The physical displacements of the disk of 0.310 inch required to produce phase changes of 180° would result in power changes and hence amplitude modulations of 1.4 percent due to the $1/R^4$ power variation. If the target were not perfectly aligned within the beam areas, these changes due to motion of the target would be larger, with correspondingly greater amplitude modulations observed. Hence, it may be concluded that rigid translational vibrations of distant targets introduce phase modulation.

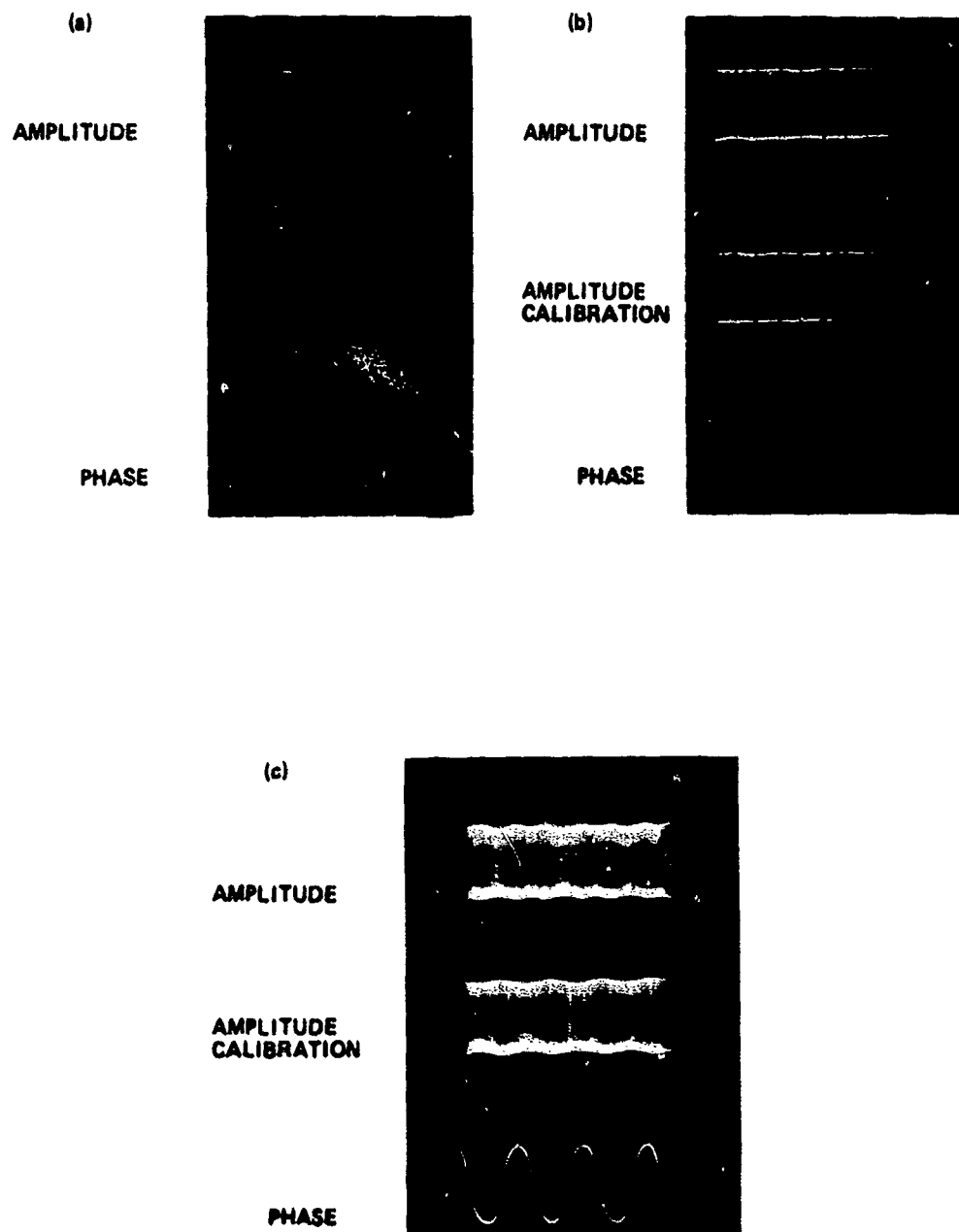


Figure 11. Measured Phase and Amplitude Modulations for Three Vibration Amplitudes: (a) 45° phase, 0 percent amplitude; (b) 90° phase, 1/2 percent amplitude; (c) 180° phase, 4 percent amplitude. (Relative amplitude vs time display)

Figure 12 shows the amount of phase modulation introduced to be independent of the vibrational frequency. The displays of Figure 12 are amplitude versus time, showing the varying d-c output of the phase detector; differing amplitudes represent differing total phase excursions. The amplitude is constant for the three different vibrational frequencies shown; additional measurements confirmed this behavior over a much wider range of frequencies.

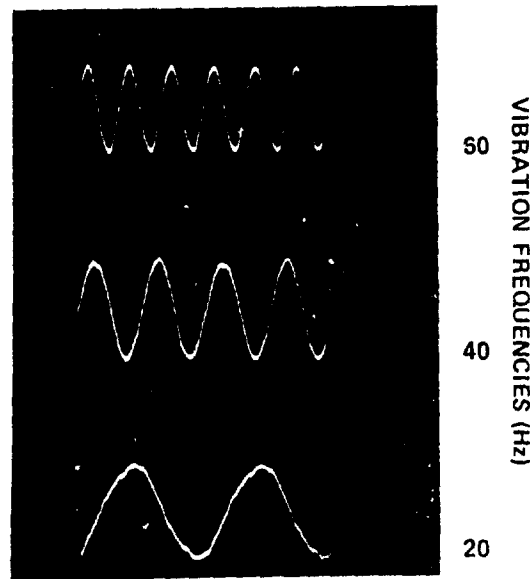


Figure 12. Phase Modulation from Constant Displacement Amplitude, Differing Vibration Frequencies (Amplitude vs time display, peak-to-peak displacement = 0.025 inch)

Figure 13 shows the amount of phase modulation introduced to be directly proportional to the amplitude of the mechanical vibration. Here, measured phase modulation is plotted against measured peak-to-peak displacements of the disk for displacements from 0.002 inch to 0.20 inch. Displacement amplitudes were measured using the General Radio Model 1553A vibration meter. The amount of phase modulation was determined by adjusting an HP precision variable phase shifter in the reference phase line to align successively the top and bottom of the sinusoidal trace with the center line of the graticule of the oscilloscope, and then subtracting the phase shifter readings corresponding to the two display positions.

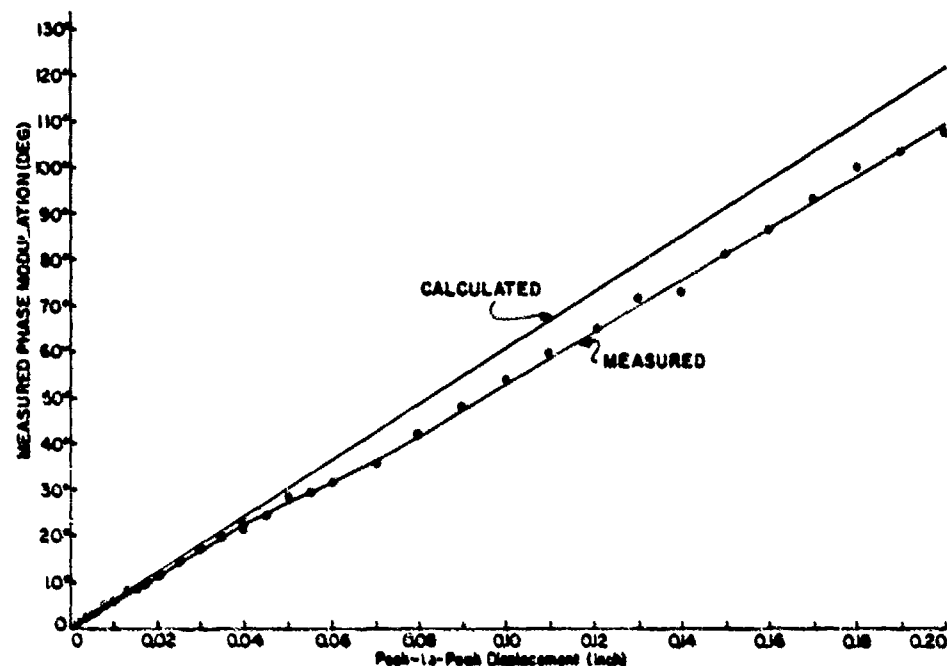


Figure 13. Measured Phase Modulation vs Vibrational Amplitude

The calculated line of Figure 13 was determined from the simple assumption that the phase shift introduced is directly proportional to the displacement of the disk. Thus,

$$\text{phase} = 360^\circ (2)(D/\lambda) \quad (3)$$

where D is the peak-to-peak displacement and λ is the wavelength, equal to 1.18 in. for the 10 GHz measurement frequency. There is agreement to within about 10 percent between the measured and calculated results, with the measured results corresponding more closely to a wavelength of about 1.33 in. The differences can most likely be attributed to nonlinearity of the phase detector or error in adjustment of the vibration meter.

An additional significant point of Figure 13 is that very small vibrational motions can be detected by examining the relative phase of the reflected signal. As shown, motions of ± 0.001 inch or $\pm 0.00085\lambda$ were readily measured with good accuracy.

Typical examples of the modulation spectra resulting from simple sinusoidal oscillation of the scatterer are given in Figure 14 for displacement amplitudes of $kd = 1$ and $kd = 2$, where $k = 2\pi/\lambda$ and d is the peak-to-peak displacement. In part (a) of Figure 14 the modulation frequency was 25 Hz and the first four maxima correspond to the fundamental and first three harmonics of the modulation frequency; the remaining maxima are due to spurious signals. In Figure 14(b) the modulation frequency was reduced to 5 Hz in order to obtain the larger required displacement corresponding to $kd = 2$ without exceeding the acceleration capabilities of the shaker. Here the first five maxima are the modulation fundamental and its first four harmonics; the remaining maxima are due to spurious signals. Relative amplitudes of the spectral components shown in Figure 14 are in good agreement with corresponding theoretical results calculated by Kleinman.²

The results of a more detailed set of measurements carried out to provide a comparison with theoretical results calculated by Kleinman are shown compared to corresponding calculated results in Figure 15, where calculated results are represented by solid lines and measured points are represented by dots and circles. The line labeled 0 represents the relative power of the radio frequency carrier; if no modulation were introduced this would be always 1, or 0 dB in the graph. The line labeled 1 represents the relative power level of the fundamental modulation frequency, and successively numbered lines represent in order the harmonics of the modulation frequency. Thus, the line labeled 4 is the third harmonic of the modulation frequency. For the measurements, the modulation frequency was 20 Hz. A vertical cut through the graph at a given value of kd gives the relative spectral levels corresponding to that vibrational amplitude; for example, a vertical line at $kd = 1$ gives the relative spectral levels of Figure 14(a).

The measured points form an independent set, and they have been normalized to the theoretical results only at $kd = 1$ on the $N = 1$ curve. Generally, agreement between calculated and measured points is very good, with some deterioration at the lower power levels.

The experimental results of Figure 15 were obtained using an H. P. Model 302A Wave Analyzer that provided an accurate amplitude comparison of the different harmonics. For high accuracy, it is particularly important to calibrate the phase detector and to adjust carefully the relative phase of the unmodulated r-f scattered and reference signals so that proper response is obtained for both odd and even harmonics.

2. Kleinman, R. E. (1975) Electromagnetic Scattering by a Linearly Oscillating Target. AFRL-TR-75-0554.

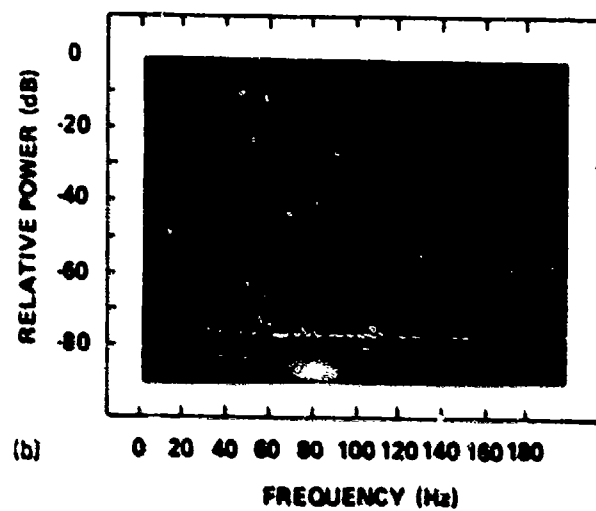
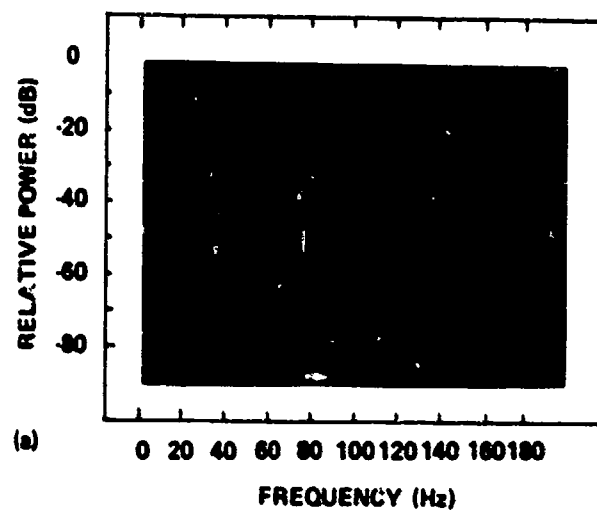


Figure 14. Modulation Spectra for Sinusoidal Oscillation of Target. (a) Displacement: $kd = 1$, $f = 25$ Hz. (b) Displacement: $kd = 2$, $f = 5$ Hz

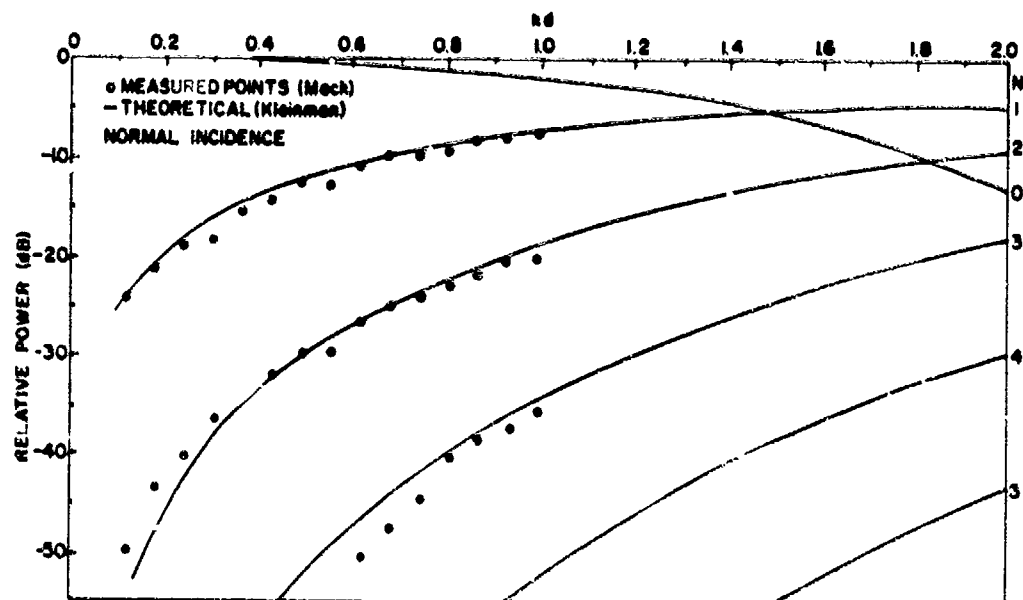


Figure 13. Comparison of Measured and Calculated Spectral Levels for Sinusoidal Vibration (Vibration frequency = 20 Hz)

References

1. Mack, R. B., Wejcieki, A. W., and Andriotakis, J. J. (1973) An Implementation of Conventional Methods of Measuring the Amplitude and Phase of Back-scatter Fields. AFCRL-TR-73-6418.
2. Kleinman, R. E. (1975) Electromagnetic Scattering by a Linearly Oscillating Target. AFCRL-TR-75-0554.

A decorative rectangular border with a repeating scroll-like pattern surrounds the central text.

MISSION of Rome Air Development Center

RADC plans and conducts research, exploratory and advanced development programs in command, control, and communications (C³) activities, and in the C³ areas of information sciences and intelligence. The principal technical mission areas are communications, electromagnetic guidance and control, surveillance of ground and aerospace objects, intelligence data collection and handling, information system technology, ionospheric propagation, solid state sciences, microwave physics and electronic reliability, maintainability and compatibility.

Printed by
United States Air Force
Hanscom AFB, Mass. 01731